Binary Fluid Mixture and Thermocapillary Effects on the Wetting Characteristics of a Heated Curved Meniscus

David M. Pratt
United States Air Force,
Wright-Patterson AFB, OH 45433-7542

Kenneth D. Kihm
Department of Mechanical Engineering,
Texas A&M University,
College Station, TX 77843-3123

An investigation has been conducted into the interactions of binary fluid mixtures (pentane [C_5H_{12}] coolant and decane [$C_{10}H_{22}$] additive) and thermocapillary effects on a heated, evaporating meniscus formed in a vertical capillary pore system. The experimental results show that adding decane, the secondary fluid that creates the concentration gradient, actually decreases the meniscus height to a certain level, but did increase the sustainable temperature gradient for the liquid-vapor interface, so did the heat transfer rate, delaying the onset of meniscus instability. The results have demonstrated that interfacial thermocapillary stresses arising from liquid-vapor interfacial temperature gradients, which is known to degrade the ability of the liquid to wet the pore, can be counteracted by introducing naturally occurring concentration gradients associated with distillation in binary fluid mixtures. Also theoretical predictions are presented to determine the magnitudes of both the thermocapillary stresses and the distillation-driven capillary stresses, and to estimate the concentration gradients established as a result of the distillation in the heated pore. [DOI: 10.1115/1.1599372]

Keywords: Binary, Evaporation, Heat Transfer, Thermocapillary, Thin Films

Introduction

Heat transport devices capable of dissipating high intensity heat energy as high as 200 W/cm^2 are required for cooling electronics; hypersonic and re-entry vehicles; satellites; propulsion and thermal energy recovery systems; cryoprobes; permafrost stabilizers; and roadway deicers among others. Of the heat transport devices presently under consideration in this regime, most utilize the latent heat of vaporization via liquid-vapor phase change. Relevant to the present research are passive capillary-driven phase change devices [1]. In these devices, the phase change occurs in a liquid-saturated porous or grooved media where capillary forces provide the driving potential for the liquid flow from the condenser to the evaporator. Ultimately for low temperature devices, the rate at which the condenser can re-supply liquid to the evaporator limits the heat transport. In practice, however, this capillary heat transport limitation is rarely achieved [2]. One possible explanation is that design predictions over-predict the wetting characteristics since they are based on a 'maximum capillary potential' which presumes that the liquid within the porous structure is perfectly wetting and static conditions exist at the evaporating menisci. Dynamic effects, other than those due to viscous flow losses, are not considered.

The speculation here is that the dynamics associated with fluid motion and heat transport in the vicinity of the evaporating meniscus can detrimentally affect the driving capillary potential by degrading the wetting ability of the working fluid [3,4]. The change in wetability is the result of non-isothermal liquid-vapor interfacial temperatures near the contact line arising from both non-uniform substrate wall temperatures and non-uniform evaporation. Either or both of these influences yield surface tension gradients on the liquid-vapor interface, with positive slope toward a cooler region of the interface. For example, if the pore wall is heated, the relatively cooler pore center region, with higher surface tension, can act to pull down the evaporating, hotter thin film region with lower surface tension. Therefore, these surface tension gradients result in thermocapillary stresses, or the pulling action, acting near the contact line which can degrade the wetability of the liquid as has been seen in many published works [5–8].

Ehrhard and Davis [5] showed that the spreading of a drop on a surface in the direction of increased wall temperature is retarded relative to the spreading of a similar drop on an isothermal surface. Furthering this work, Hocking [6] showed that the advancement or spreading of an evaporating drop is retarded due to the evaporation process. Sen and Davis [7] showed that, for a slot configuration, surface tension gradients create a fluid surface flow field, which also affects the liquid wetability. Anderson and Davis [8] analytically demonstrated that the flow field was coupled to the temperature field through the thermocapillarity as discussed by Sen and Davis [7].

Recent studies of rewetting of liquids along inclined heated plates by Ha and Peterson [9] and Chan and Zhang [10] showed that the maximum wicking height measured was beneath that predicted using the typical Laplace-Young equation by as much as thirty percent. Pratt and Hallinan [4] established and experimentally verified the relationship between the liquid-vapor interfacial temperature gradient and the wetting characteristics of a liquid within small pores. They showed that thermocapillary stresses acting near the contact line of the advancing liquid front inhibit the wetting of the liquid thereby reducing the wicking height.

The predicted degradation leads to a reduction in the capillary pumping potential in capillary heat transfer devices and thus a reduction in their ability to transport energy [2]. Thus the question arises as to how to minimize this reduction. The degradation arises from thermocapillary stresses along the liquid-vapor interface due to the reduction in surface tension with an increase in temperature. One possible solution to counteract the degradation is the introduction of a small amount of a relatively high surface-free-energy, less volatile fluid (additive) into the volatile or relatively low surface-free-energy working fluid. This would result in an increase in the concentration of the less volatile fluid with an increase in temperature or the preferred evaporation of the lower

Contributed by the Heat Transfer Division for publication in the JOURNAL OF HEAT TRANSFER. Manuscript received by the Heat Transfer Division November 22, 2002; revision received May 16, 2003. Associate Editor: G. P. Peterson.

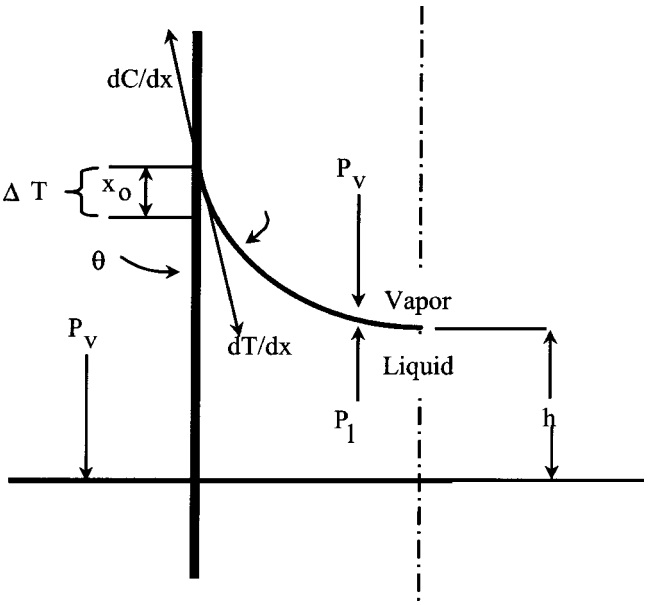

Fig. 1 Liquid-vapor interface of a binary mixture working fluid with heated pore wall

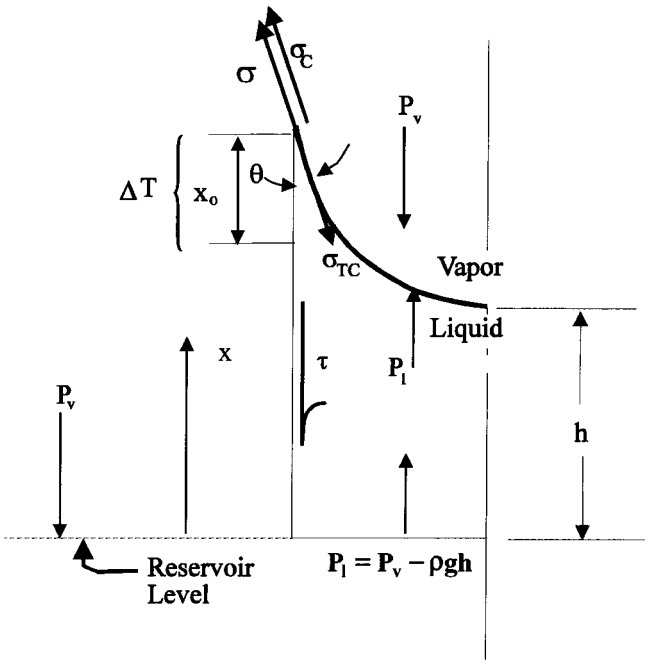

Fig. 2 Binary mixture meniscus inside a capillary tube with an induced temperature gradient by wall heating and a concentration gradient by distillation of a more volatile working fluid

surface-free-energy fluid. This would thus result in a concentration gradient for additive in the opposite direction to the temperature gradients (see Fig. 1), and the additive concentration gradient is consistent with the surface tension gradient of the mixture, so-called distillation effect [11], which counteracts the thermocapillary surface tension gradient.

The distillation effects of binary mixtures for the case of superheated or pool boiling cases have been examined by several researchers [12–14]. Reddy and Lienhard [12] presented an observation of the presence of induced subcooling because of composition differences that makes the liquid bulk temperature lower than the vapor temperature. Avedisian and Purdy [13] reported the critical boiling heat flux for pentane-heptane and pentane-propanol binary mixtures under different saturation pressures. Parks and Wayner [11] presented an anlytical model to predict the meniscus profiles near the contact line for a binary mixture and showed an experimental validation. Their model also showed that the single most important mechanism for flow in the microscale evaporating meniscus region of 1 to 10 μm thickness is the distillation-driven capillary stress resulting from preferential evaporation of the more volatile component. Reyes and Wayner [14] presented an interfacial model to predict the critical heat flux for various binary mixtures and to compare their predictions with published experimental data.

The present paper reports an experimental investigation that was designed so that macroscopic wetting characteristics could be observed for a heated and evaporating meniscus within a simple capillary pumped loop. Specifically, it was designed to determine the effects of binary fluid mixtures (pentane [C_5H_{12}] coolant and decane [$C_{10}H_{22}$] additive) on the thermocapillary stresses arising near the contact line of evaporating menisci, within capillary pores, by measuring the capillary pumping potential or the meniscus height differentials between the evaporator and condenser cores. In addition, a preliminary analysis has been conducted to examine the range of the parametric requirements to ensure an ideal counter-balancing between the thermocapillary stress and the distillation-driven capillary stress.

Analysis

Analysis is presented to qualitatively explain the experimental results, rather than as a rigorous solution to the problem herein discussed. The most easily measurable macroscopic wetting characteristic of a liquid in a pore is the wicking height. For static interfacial conditions, it can be predicted with the Young-Laplace equation [15].

$$P_v - P_l = \sigma K \tag{1}$$

The reduced liquid pressure at the meniscus causes the liquid to wick to a height h (Fig. 2), which for an axisymetric pore of radius r and a condenser of radius R gives rise to the following expression

$$\rho g h = \frac{2\sigma(R-r)}{rR}\cos\theta \tag{2}$$

where θ is the apparent contact angle and σ is the surface tension of the mixture. When the meniscus is heated via wall heating, dynamic effects can alter this wicking height.

One effect of heating is to produce a liquid-vapor interfacial temperature gradient near the contact line, with a negative slope toward the pore center. This temperature gradient gives rise to a thermocapillary stress (σ_{TC}) emanating from the contact line if the contact line region is hotter than the remainder of the meniscus. Additionally, the evaporative transport from the meniscus due to the heat transfer induces liquid flow from the bulk pore region. Associated with this flow are viscous losses (τ) along the wall of the pore. The use of a binary fluid mixture gives rise to an additional stress along the interface resulting from the naturally occurring concentration gradient which tends to counteract the thermocapillary stress, because of the aforementioned distillation effect. While, both the thermocapillary and the flow loss effects can reduce the wicking height, the concentration effect acts to negate these effects.

A vertical force balance is applied to the control volume defined by the liquid column in the pore shown in Fig. 2 to determine the thermocapillary and flow loss effects on capillary potential. This results are in the following equilibrium condition.

$$(P_l - P_v)\pi r^2 + (\sigma - \sigma_{TC} + \sigma_C)2\pi r\cos\theta - \Delta P_{\text{flow}}\pi r^2 - \sigma 2\pi R\cos\theta = 0 \tag{3}$$

with $P_l - P_v = -\rho g h$. Dividing by πr^2 and substituting yields

$$\rho g h = \frac{2(\sigma - \sigma_{TC} + \sigma_C)}{r}\cos\theta - \frac{2\sigma R}{r^2}\cos\theta - \Delta P_{\text{flow}} \tag{4}$$

Elementary momentum analysis assuming fully-developed laminar pipe flow of radius r gives an expression for the pressure differential for the flow length L_{flow} measured from the bottom of the capillary tube to the meniscus as,

$$\Delta P_{\text{flow}} = \frac{8\mu\langle V\rangle}{r^2} L_{\text{flow}} \tag{4a}$$

Considering the energy balance between the heat input to meniscus Q_M and the evaporative mass flow rate $\dot{m}_{\text{evap}}$, the average flow velocity $\langle V\rangle$ is expressed as,

$$\langle V\rangle = \frac{Q_M}{\rho A[h_{fg} + c_p \Delta T]} \tag{4b}$$

where the cross-sectional area $A \equiv \pi r^2$ and the temperature differential, $\Delta T \equiv T_{\text{sat}} - T_r$, is set between the saturation condition at the evaporating interface and the reservoir condition at the bottom of the capillary bulk. Combining Eqs. (4*a*) and (4*b*) gives

$$\Delta P_{\text{flow}} = \frac{8\mu L_{\text{flow}}}{\rho\pi r^4} \frac{Q_M}{h_{fg} + c_p(T_{\text{sat}} - T_r)} \tag{4c}$$

Substituting Eq. (4*c*) into Eq. (4) yields

$$\rho g h = \frac{2(\sigma - \sigma_{TC} + \sigma_C)}{r}\cos\theta - \frac{2\sigma R}{r^2}\cos\theta - \frac{8\mu L_{\text{flow}}}{\rho\pi r^4} \frac{Q_M}{h_{fg} + c_p(T_{\text{sat}} - T_r)} \tag{5}$$

This modified version of the capillary pumping potential incorporates yet undefined thermocapillary and concentration forces that can be determined by examining the effects of liquid-vapor interfacial temperature gradients on the surface tension. Assuming the mixture surface tension is linearly contributed by the mixture concentration,

$$\sigma = C(\sigma_{oD} - \gamma_D T) + (1 - C)(\sigma_{oP} - \gamma_P T) \tag{6}$$

so that letting

$$\sigma_C - \sigma_{TC} = \frac{\partial \sigma}{\partial x} x_o \tag{7}$$

and differentiation of Eq. (6) with respect to x gives,

$$\frac{\partial \sigma}{\partial x} = \frac{\partial C}{\partial x}(\sigma_{oD} - \gamma_D T - \sigma_{oP} + \gamma_P T) - \frac{\partial T}{\partial x}[C\gamma_D + (1 - C)\gamma_P] \tag{8}$$

Finally expressions for the thermocapillary and concentration forces are obtained from combining Eqs. (7) and (8) as,

$$\sigma_{TC} = \frac{\partial T}{\partial x}[C\gamma_D + (1 - C)\gamma_P] x_o \tag{9}$$

and

$$\sigma_C = \frac{\partial C}{\partial x}[(\sigma_{oD} - \gamma_D T) - (\sigma_{oP} - \gamma_P T)] x_o \tag{10}$$

The thermocapillary stress, Eq. (9), is of the same form as that which was shown to exist by Pratt and Hallinan [4].

For an ideal case, the thermocapillary stress (Eq. (9)) can be completely counteracted by the distillation-driven capillary stress (Eq. (10)), i.e.,

Table 1 Decane concentration at the meniscus top (C_T) for complete counteraction of the distillation-driven capillary to the thermocapillary drive: for different decane concentrations at the meniscus bottom, (C_B), and for different temperature gradients along the meniscus, ($\partial T/\partial x$) = 10^2, 10^3, 10^4, 3×10^4 and 6×10^4.

$\partial T/\partial x$ (K/m)	Decane Concentration at the Meniscus Bottom or Bulk Mixture (C_B)			
	0.01	0.03	0.05	0.1
10^2	0.01145	0.03145	0.05145	0.10145
10^3	0.0245	0.0445	0.0645	0.1145
10^4	0.155	0.175	0.195	0.245
3×10^4	0.445	0.465	0.485	0.535
6×10^4	0.867	0.887	0.907	0.957

$$\frac{\sigma_{TC}}{\sigma_C} = \frac{\dfrac{\partial T}{\partial x}[C\gamma_D + (1 - C)\gamma_P]}{\dfrac{\partial C}{\partial x}[(\sigma_{oD} - \gamma_D T) - (\sigma_{oP} - \gamma_P T)]} = 1 \tag{11}$$

where the ratio of the temperature gradient to the concentration gradient must be ensured as,

$$\Re_{T-C} \equiv \frac{\dfrac{\partial T}{\partial x}}{\dfrac{\partial C}{\partial x}} = \frac{[(\sigma_{oD} - \gamma_D T) - (\sigma_{oP} - \gamma_P T)]}{[C\gamma_D + (1 - C)\gamma_P]} \tag{12}$$

Note that the required ratio $\Re_{T-C}$ varies with the mixture temperature T and decane concentration C.

Assuming a linear change in the decane concentration from C_B at the meniscus bottom point, or equivalent to the bulk mixture concentration, to C_T at the meniscus upper end,

$$C_T = \left(\frac{\partial C}{\partial x}\right) r + C_B \tag{13}$$

For a specified ($\partial T/\partial x$), ($\partial C/\partial x$) is given from Eq. (12) and the concentration differential $C_T - C_B$ can be calculated from Eq. (13). Table 1 shows example calculations for C_T for different C_B for the range of ($\partial T/\partial x$) from 10^2 to 6×10^4, where a constant value of $\Re_{T-C} = 70.0$ is used assuming $T = 290$ K. To be shown later in Results Section, temperature gradient along the meniscus surface, $\partial T/\partial x$ for the present experiment spans up to 10^4 or less for all cases of C_B. Note that the decane concentration differential $C_T - C_B$ increases linearly with increasing $\partial T/\partial x$, as expected.

Experiment

To accomplish the goal of the research, a single pore capillary pumped heat transfer device was constructed as shown in Fig. 3. The test specimen shown is a closed, single pore evaporator capillary pumped loop consisting of a pore evaporator of 2 mm diameter with 10 mm diameter pore condensers. This idealized and enlarged evaporator was designed to study some basic physics that can be extracted for potential applications to the meniscus development in an individual pore of a porous structure of heat pipes and capillary pumps.

Heat is introduced via electrical resistance heating elements mounted on the outer diameter of the evaporator pore. To minimize convection losses and isolate the test specimen, shown in Fig. 3, from ambient conditions, it was placed in a vacuum chamber (Fig. 4). The chamber was equipped with feed-throughs for thermocouples, pressure transducers, heater power connections, and cooling fluid lines.

A roughing vacuum pump was used to evacuate the loop system and the vacuum chamber. The filling of the test loop system uti-

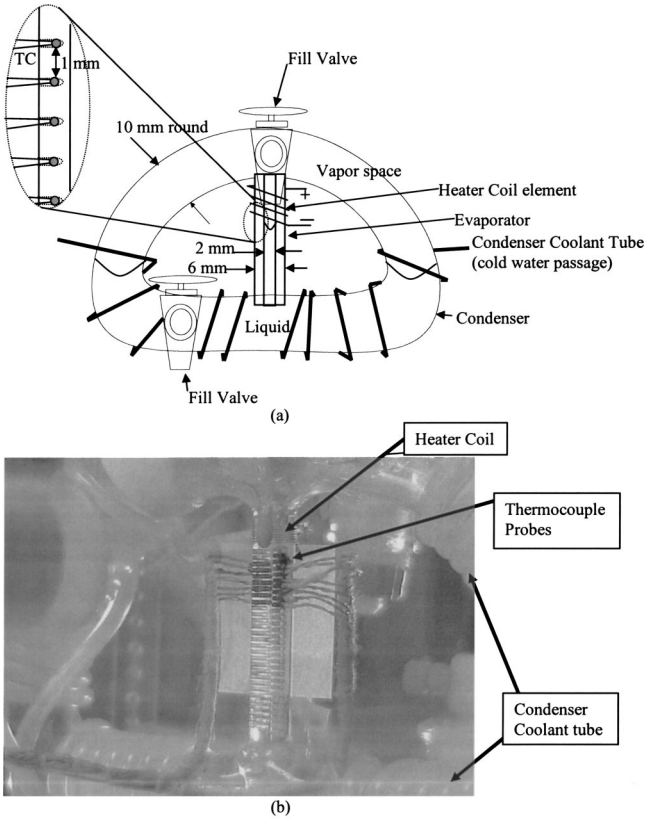

Fig. 3 Schematic of the single pore capillary pumped loop

lizes a large fluid reservoir filled with the appropriate ratio of working fluids. This reservoir is connected to the test specimen and a vacuum pump through complex plumbing that allows vacuum to be pulled from the specimen and the reservoir and regulation of the fluid fill to the specimen. All of these processes are controlled independently so that the amount of charging can be adjusted. The working fluid consisted of a binary fluid mixture of n-pentane and decane. The properties for which are presented in Table 2. Concentrations of 0, 3, 5, and 10% by volume of decane were examined. To control the temperature of the condenser region, a refrigerated circulator was used to pump a constant temperature cooling fluid through the coolant tube wrapped around the exterior of the condenser region.

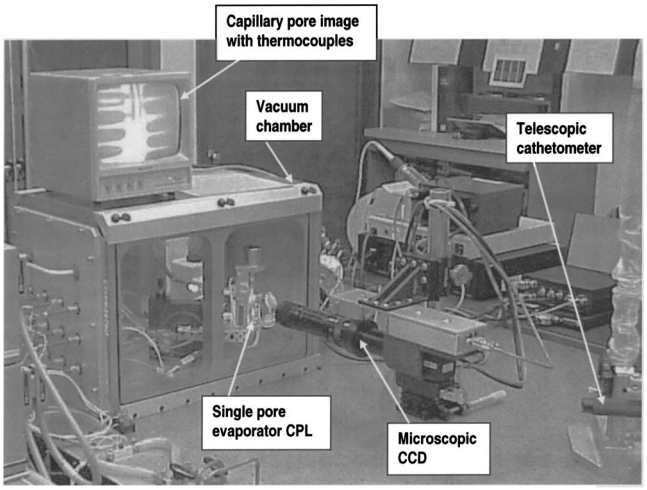

Fig. 4 Experimental setup of the single pore evaporator capillary pumped loop (CPL) placed in a vacuum chamber

Table 2 Properties of Pentane and Decane

Pentane (C_5H_{12}) (Working fluid)	Decane ($C_{10}H_{22}$) (Additive)
$M=72.15$	$M=142.28$
$\sigma=0.0155$ N/m (at 20°C)	$\sigma=0.0234$ N/m (at 20°C)
$\sigma_{op}=0.04835$ N/m	$\sigma_{od}=0.05079$ N/m
$\gamma_p=0.0001102$ N/m·K	$\gamma_d=0.00009197$ N/m·K
Refractive index (n) $=1.3545$ at 20°C	Refractive index (n) $=1.4102$ at 20°C
$T_{BOIL}=36.1$°C at 1 atm	$T_{BOIL}=174.1$°C at 1 atm
$\rho=621.4$ kg/m^3	$\rho=726.4$ kg/m^3

Calibrated thermocouples were used to measure the wall temperature of the capillary tube and to measure the temperature of the vapor path and liquid reservoir at the condenser. To determine the temperature distribution of the evaporator region, thermocouples with 0.25 mm bead size were positioned at 0.5 mm intervals along the capillary pore. This was accomplished by creating two rows of thermocouples 180 deg apart. Each row had thermocouples placed longitudinally every millimeter and the two rows have a longitudinal offset of 0.5 mm. Data were recorded using an A/D board interfaced to a Pentuim III—500 PC. The associated errors in the temperature readings were ±0.3°C with a 95% confidence interval. A video microscope system was used to image the meniscus profile so that the contact angle could be estimated. It consisted of a long distance microscope connected to a Hi-8 resolution black and white camera. This image was recorded using an SVHS video recorder. The meniscus was back lit with a high intensity white light source, filtered to allow transmission of light in the green spectrum only and to block transmission of much of the thermal radiation in the infrared spectrum.

The refrigerated circulator temperature was used to set the liquid reservoir (condenser) temperature at 5, 15, and 25°C. Tests were run for each of these system states for variable heat input. The test conditions and power input for the tests are summarized in Table 3. The data presented in this table includes the bulk liquid reservoir temperature and the range of the considered power input.

The capillary tube was heated using a fine Nichrome heater wire (spirally wrapped around the tube at the top) having a resistance of 1 Ω/cm. It was connected to a precision DC power supply capable of producing up to three amps at thirty volts. A shunt resistor connected in series with the heating element allowed for the current flowing through the heater to be determined by measuring the voltage drop across it.

Table 3 Experimental test conditions

Volume concentration of Decane (%)	Condenser temperature (°C)	Heat input (W)
0	5	0–1.4
	15	0–1.4
	25	0–1.4
3	5	0–2.7
	15	0–2.6
	25	0–3
5	5	0–2.1
	15	0–2.4
	25	0–2.4
10	5	0–1.8
	15	0–3
	25	0–3

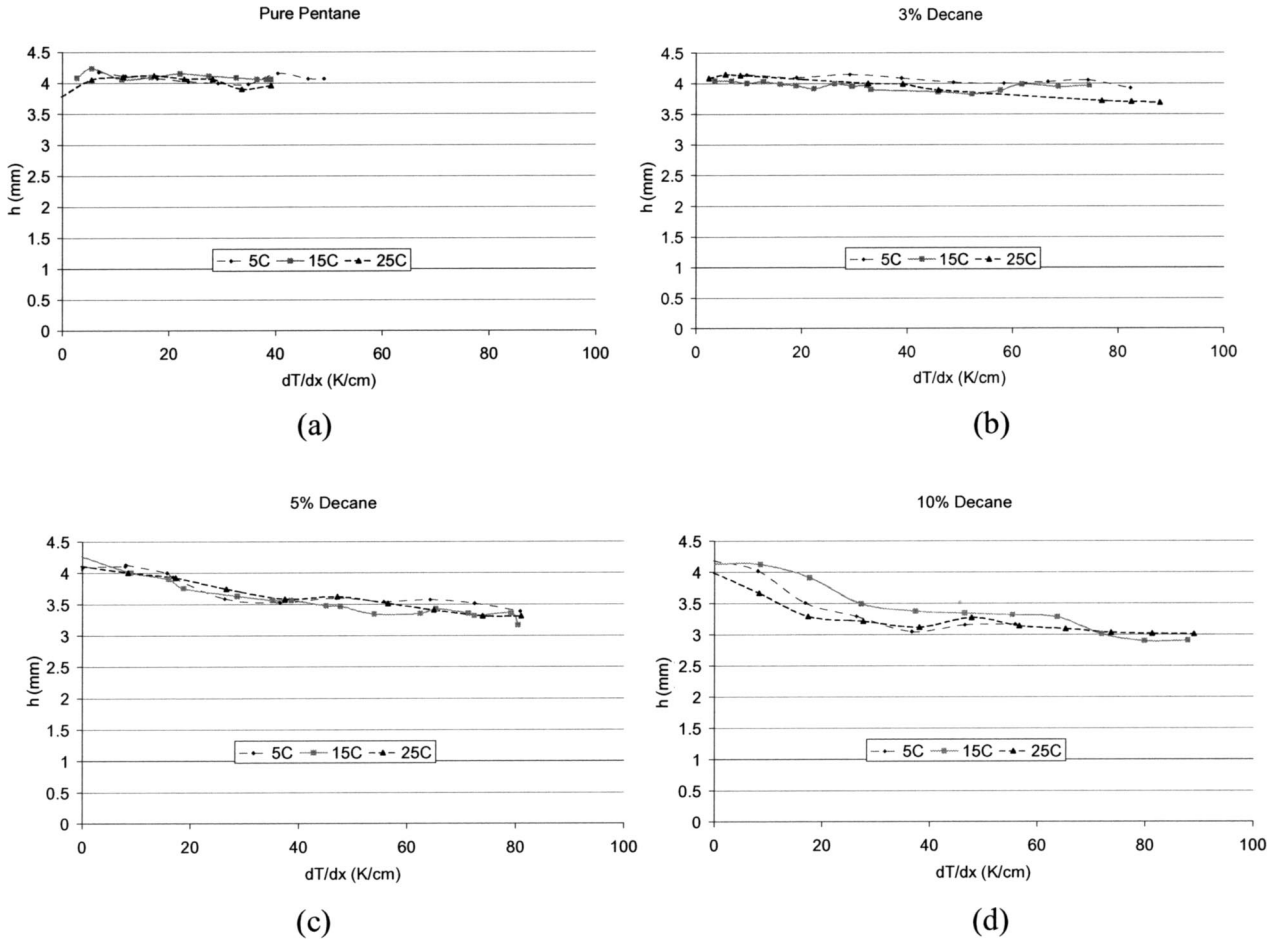

Fig. 5 Capillary pumping potential versus wall temperature gradient: (a) Pure pentane, (b) 3% decane, (c) 5% decane, and (d) 10% decane in volume in the mixture with pentane.

Results

For full examination of the experimentally determined wetting characteristics, data is presented for the conditions detailed in Table 3. This presented data includes the steady-state wicking height versus wall temperature gradient for concentrations of 0, 3, 5, and 10% decane in volume in the mixture with pentane. The capillary pumping potential, or equivalent to the wicking height differential between the evaporator and condenser pores, was measured by a cathetometer that essentially consists of a small telescope with a horizontal hairline to be adjusted in height with the meniscus bottom location and has a digital meter with minimum reading resolution of ± 5 μm. For each measurement condition, up to thirty (30) readings were averaged to alleviate the uncertainties associated with the potentially subjective reading variations through the cathetometer.

Tests were conducted until the temperature nearest to the heating element exceeded 110°C or for the pure pentane case, the system became dynamically unstable. The *x*-axis on all plots is set to the same scale to assist in comparisons. Total errors associated with these plots are $\pm 2.7\%$ with a 95% confidence interval for the capillary pumping potential measurements, and $\pm 8.5\%$ at a 95% confidence interval for the temperature gradient assessment.

Figure 5 is a presentation of capillary pumping potential versus wall temperature gradient at the meniscus for 0 (pure pentane), 3, 5, and 10% decane in volume. All binary mixtures show significantly extended temperature gradients with the onset of meniscus instability deferred in that meniscus said to be unstable when oscillatory motion occurs. The temperature gradient dT/dx is determined from the thermocouple readings that are located closest to the meniscus so that it can be approximated to be comparable to the temperature gradient along the interface [16,17]. Note that the measurements were stopped once any of the thermocouple readings reached 110°C to prevent thermally induced cracking of the glass pore and the stable operation ranges could span farther allowing higher temperature gradients than presented. It shows that there is little variation in wicking height with subcooling of the condenser temperature for all the cases examined.

In Fig. 6 the same data sets are re-grouped and re-plotted so that the effect of the decane concentration on the capillary pumping potential can be more exclusively observed. These show that for low concentrations of decane the capillary pumping potential is not deleteriously affected. However for high concentrations of decane the wicking height, i.e., capillary pumping potential is drastically reduced, whereas their stable operational ranges have been significantly extended. This is a result of the distillation process near the contact line where decane is the primary component and thus dominates the wetting characteristics or contact angles. To understand the significance of this assumption, examination of the contact angle is required.

Figure 7 is a semi-empirical plot of contact angle versus liquid temperature. The values presented were obtained by measuring the wicking height of a single pore placed within a large liquid reservoir held at a known temperature and calculating the contact angle using Eq. (14).

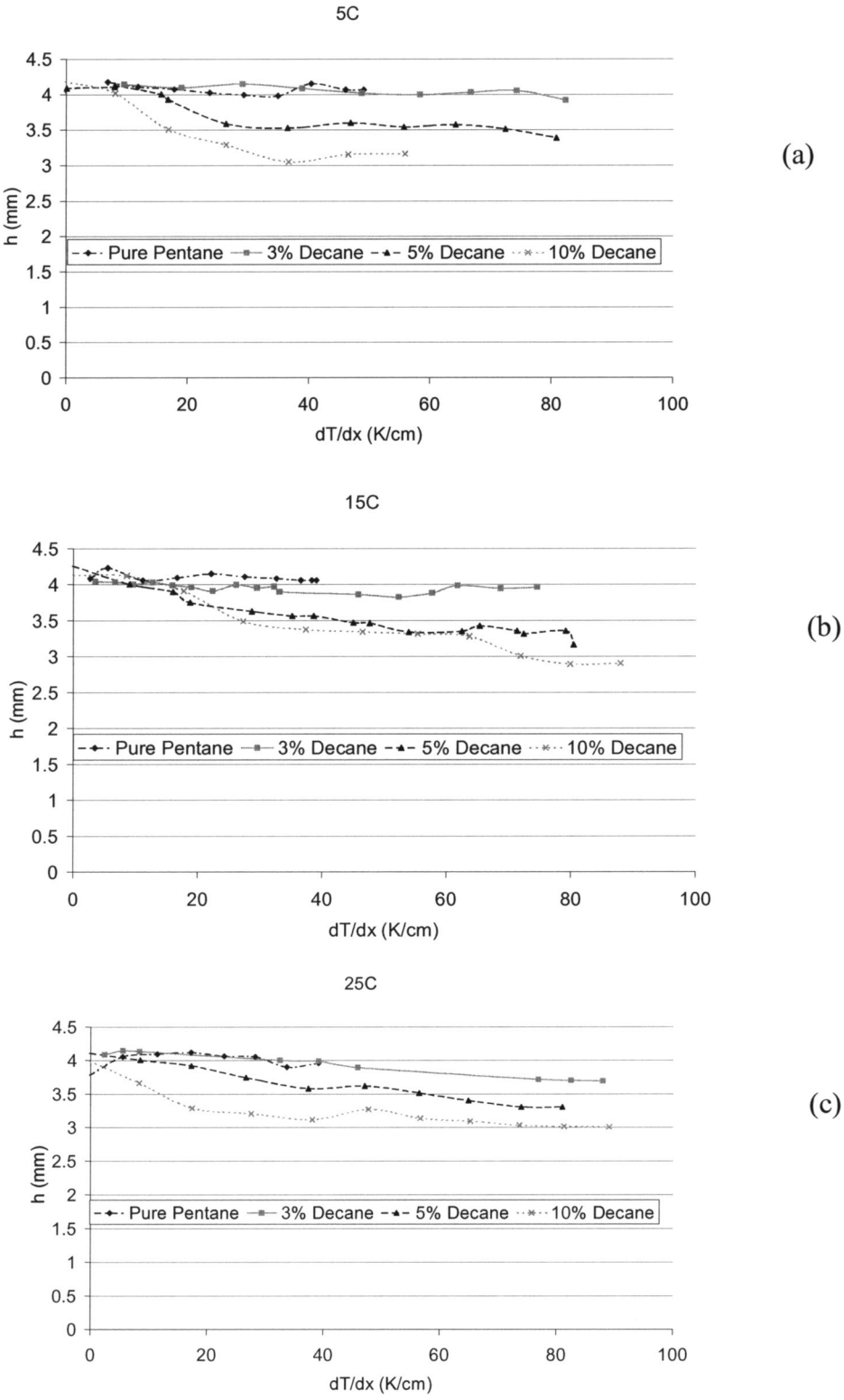

Fig. 6 Capillary pumping potential versus wall temperature gradient for decane concentrations: (a) condenser temperature at 5°C, (b) 15°C, and (c) 25°C.

$$\theta = \cos^{-1} \frac{\rho g h r}{2\sigma} \tag{14}$$

Then the Young-Dupre' equation (Eq. (15)) was applied to determine the variation in contact angle with temperature by assuming that the numerator was approximately constant with temperature for the tested range and allowing the denominator to vary.

$$\cos\theta = \frac{\sigma_{sv} - \sigma_{sl}}{\sigma} \tag{15}$$

The produced contact angle data was then used in Eq. (2) to examine the variation in wicking height due solely to bulk liquid temperature variations for pure pentane, and a decane in pentane mixture where a decane dominated contact angle is expected (Fig.

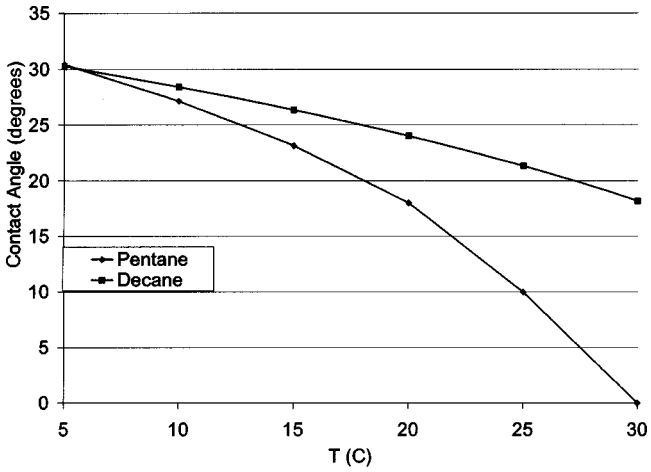

Fig. 7 Contact angle versus liquid temperature for pure pentane and pure decane

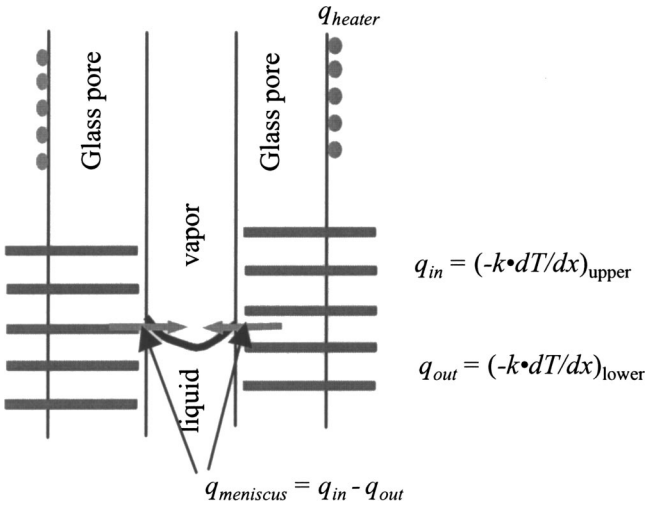

Fig. 10 Energy balance at the meniscus to estimate the amount of heat transfer into the meniscus

8). For pure pentane, the contact angle calculated for pentane was used, and for the mixture, the contact angle measured for decane was used because of the distillation effect is prevalent near the heated wall. The results show similar variations in wicking height as those seen during testing. Thus the assumption that for high decane concentration mixtures, the decane controls the contact angle, seems to be substantiated. This also supports the model developed and presented in Eqs. (8) to (10) because if the wicking height variation is due to changes in contact angle, no net interfacial stress exists. This is apparent if the model is examined. It shows that the thermocapillary stress is balanced by the stress arising from the concentration gradient along the liquid-vapor interface. This balance would yield no net interfacial stress.

Finally, consideration must be made as to how if at all the addition of decane to the working fluid affects heat transfer. To do this two variables must be examined, (1) the rate of energy consumed for evaporation at the meniscus, and (2) the temperature of the meniscus. Figure 9 shows the power input into the meniscus versus the total power provided for the electric heater versus 0, 3, 5, and 10% decane in volume in the mixture with pentane and for a fixed 25°C condenser temperature. This figure shows that the addition of decane into the pentane has no degrading effect on the energy transferred into the meniscus. The heat transferred into the meniscus is calculated by applying a simple energy balance at the meniscus location from the thermocouple data, as illustrated in Fig. 10. This may represent a slightly overestimated heat transfer rate to the meniscus in that the direct heating from the glass inner pore wall to the vapor and to the bulk liquid regions is not accounted for. However, those direct or convective heating magni-

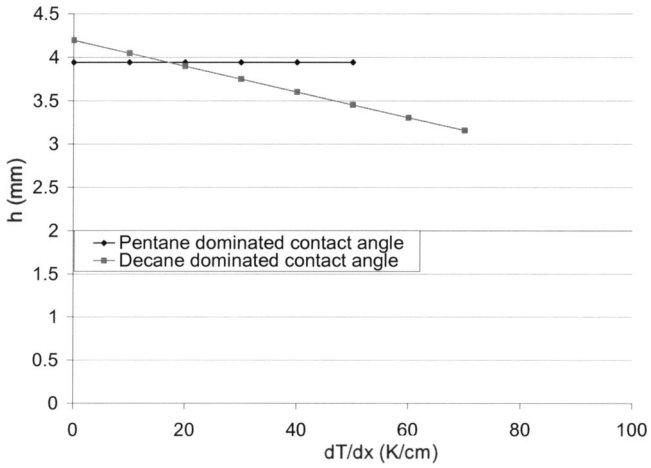

Fig. 8 Capillary pumping potential versus wall temperature gradient

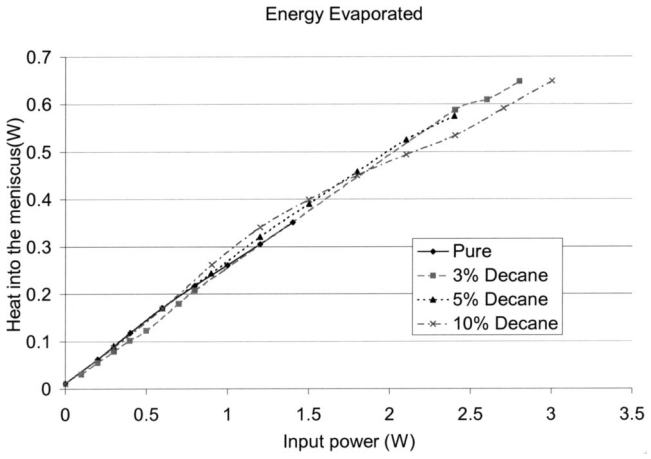

Fig. 9 Heat transferred into the meniscus versus total heat input for a fixed condenser temperature of 25°C

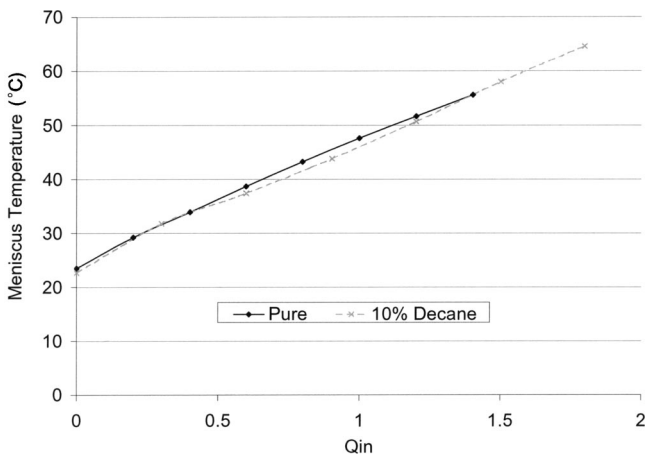

Fig. 11 Temperature at the meniscus versus input power-condenser temperature is 25°C

tudes will not be substantial because of small temperature differentials at the solid-bulk liquid and solid-vapor interfaces and the majority of heat transfer is taking place in the meniscus region under evaporation.

To further substantiate this conclusion, examination of the aforementioned second variable, the meniscus temperature is necessary. Figure 11 is a presentation of the temperature of the thermocouple closest to the intrinsic meniscus for the two limiting cases of pure pentane and 10% decane in pentane. Figure 11 shows that there is no significant variation in the temperature at the meniscus for the two limiting cases. This in conjunction with Fig. 9 demonstrates that the heat transfer characteristics of the system are not necessarily depreciated due to the addition of decane, while the range of stable establishment of its capillary pumping potential is significantly extended in terms of the temperature gradient at the meniscus.

Conclusions

Analysis describing a novel method of negating the deleterious effects of thermocapillary stress on capillary driven phase change devices has been presented and preliminary experiments have been completed, showing its validity. The data revealed that added concentrations of decane in pentane warrant that the onset of meniscus instability is noticeably prolonged with no degradation in heat transfer. This improvement is attributed to concentration-driven capillary gradient due to the distillation of the pentane in the near contact line region, which counteracts the degrading thermocapillary pulling actions, along the meniscus. However, for high concentrations of decane in pentane, substantial reductions in wicking height were observed due to the higher surface-free-energy as decane dominates the contact angle characteristics. Nevertheless, neither the rate of heat input to meniscus nor the meniscus temperature shows any noticeable degradation with the wicking height reduction.

Acknowledgment

This material is based on the work partially supported by the National Research Council-Summer Faculty Fellow Program (SFFP) for Dr. K. D. Kihm and by the Air Force Office of Scientific Research Laboratory Research Initiation Request. Any opinions, findings, and conclusions or recommendations expressed in this publication are those of the authors and do not necessarily reflect the view of the NRC or the AFOSR.

Nomenclature

C = volumetric concentration of decane
c_p = constant pressure specific heat (J/kg-K)
g = acceleration due to gravity (m/s^2)
h = wicking height (m)
h_{fg} = latent heat of vaporization (J/kg)
K = curvature (1/m)
L = length (m)
M = molecular mass
n = index of refraction
P = pressure (Pa)
r = radius of the capillary tube (m)
R = radius of the condenser (m)
T = temperature (°C)
V = average liquid velocity (m/s)
x = cartesian coordinate parallel to thin film (m)
$\Re_{T-C}$ = ratio of the temperature gradient to the concentration gradient [Eq. (12)]
γ = slope of surface tension (N/m-K)
μ = absolute viscosity (Pa-s)
θ = contact angle (degrees)
ρ = density (kg/m^3)
σ = surface tension (N/m)

Subscripts

B = bottom of meniscus
C = concentration
D = decane
flow = flow
l = liquid
o = reference
P = pentane
r = reservoir
sat = saturation
sl = solid-liquid
sv = solid-vapor
T = top of meniscus
TC = thermocapillary
v = vapor

References

[1] Chang, W. S., and Hager, B. G., 1990, ''Advance Two-Phase Thermal Management in Space,'' *National Heat Transfer Conference*, Minneapolis, MN.
[2] Pratt, D. M., Chang, W. S., and Hallinan, K. P., 1998, ''Effects of Thermocapillary Stresses on the Capillary Limit of Capillary-Driven Heat Transfer Devices,'' *Proc. 11th International Heat Transfer Conference*, Kyongju, Korea.
[3] Ma, H. B., Pratt, D. M., and Peterson, G. P., 1998, ''Disjoining Pressure Effect on the Wetting Characteristics in a Capillary Pore,'' Microscale Thermophys. Eng., **2**(4), pp. 283–297.
[4] Pratt, D. M., and Hallinan, K. P., 1997, ''Thermocapillary Effects on the Wetting Characteristics of a Heated Curved Meniscus,'' J. Thermophys. Heat Transfer, **11**(4), pp. 519–525.
[5] Ehrhard, P., and Davis, S. H., 1991, ''Non-Isothermal Spreading of Liquid Drops on Horizontal Plates,'' J. Fluid Mech., **229**, pp. 365–388.
[6] Hocking, L. M., 1995, ''On Contact Angles in Evaporating Liquids,'' Phys. Fluids, **7**(12), pp. 2950–2955.
[7] Sen, A. K., and Davis, S. H., 1982, ''Steady Thermocapillary Flows in Two-Dimensional Slots,'' J. Fluid Mech., **121**, pp. 163–186.
[8] Anderson, D. M., and Davis, S. H., 1994, ''Local Fluid and Heat Flow Near Contact Lines,'' J. Fluid Mech., **268**, pp. 231–265.
[9] Ha, J. M., and Peterson, G. P., 1994, ''Analytical Prediction of the Axial Dryout Point for Evaporating Liquids in Triangular Microgrooves,'' ASME J. Heat Transfer, **116**(2), pp. 498–503.
[10] Chan, S. H., and Zhang, W., 1994, ''Rewetting Theory and the Dryout Heat Flux of Smooth and Grooved Plates With a Uniform Heating,'' ASME J. Heat Transfer, **116**(1), pp. 173–179.
[11] Parks, C. J., and Wayner, Jr., P. C., 1987, ''Surface Shear Near the Contact line of a Binary Evaporating Curved Thin Film,'' AIChE J., **33**(1), pp. 1–10.
[12] Reddy, R. P., and Lienhard, J. H., 1989, ''The Peak Boiling Heat Flux in Saturated Ethanol-Water Mixtures,'' ASME J. Heat Transfer, **111**, pp. 480–486.
[13] Avedisian, C. T., and Purdy, D. J., 1993, ''Experimental Study of Pool Boiling Critical Heat Flux of Binary Fluid Mixtures on an Infinite Horizontal Surface,'' *Proceedings of 1993 ASME International Electronics Packaging Conference*, **2**, pp. 909–915.
[14] Reyes, R., and Wayner, P. C., 1997, ''Interfacial Models for the Critical Heat Flux Superheat of a Binary Mixture,'' National Heat Transfer Conference, HTD-Vol., 342, pp. 187–194.
[15] Carey, V. P., 1999, *Statistical Thermodynamics and Microscale Thermophysics*, Cambridge University Press, Cambridge, UK, Chap. 10.
[16] He, O., 1996, ''Novel Microscale Flow Field Measurement Technique for Extracting Fundamental Physics of Dynamic Thin Films,'' Ph.D. dissertation, Dept. of Mechanical and Aerospace Engineering, Univ. of Dayton, Dayton, OH.
[17] Pratt, D. M., Brown, J. R., and Hallinan, K. P., 1998, ''Thermocapillary Effects on the Stability of a Heated, Curved Meniscus,'' ASME J. Heat Transfer, **120**, pp. 220–226.